Acta Astronautica 210 (2023) 627–634

Contents lists available at ScienceDirect

Acta Astronautica

journal homepage: www.elsevier.com/locate/actaastro

Self-healing polymers for space: A study on autonomous repair performance and response to space radiation

Laura Pernigoni [a,*], Ugo Lafont [b], Antonio M. Grande [a]

[a] Department of Aerospace Science and Technology, Politecnico di Milano, via La Masa 34, 20156, Milan, Italy
[b] European Space Research and Technology Centre, European Space Agency, Keplerlaan 1, PO Box 299, 2200 AG Noordwijk, the Netherlands

ARTICLE INFO

Keywords:
Self-healing polymers
Space radiation
Composites
Inflatable space structures

ABSTRACT

One of the main challenges of space exploration is to properly protect astronauts from the hazards of the space environment. Space suits were hence created to protect crewmembers during extravehicular activities, but they are currently unable to properly withstand damage after, for example, impacts with micrometeoroids and orbital debris (MMOD), and they would depressurize and collapse if punctured, with catastrophic consequences. In this context, the possibility of integrating self-healing materials into spacesuits has drawn the attention of the scientific community, as it would lead to autonomous damage restoration and subsequently increased safety and operational life. Nevertheless, the effects of space environment on these materials are still to be determined and could lead to a significant decrease of their overall performance.

The here presented study focuses on a first example of application to a space suit, analyzing the healing performance of a set of candidate self-healing polymers before and after exposure to simulated space radiation. A comparison of bilayers and nanocomposites having these polymers as matrices is also made in the non-irradiated case. This research also aims at filling the gap between standard characterization of self-healing materials (e.g.: scratch, impact, and puncture tests) and assessment of the effects of space radiation on them by combining these two aspects. Understanding if and how radiation can affect damage recovery performance is in fact fundamental to determine whether a given self-healing material can actually be used for space applications.

The self-healing response is assessed through in-situ flow rate measurements after puncture damage. Maximum and minimum flow rate, the time between them and the air volume lost within the 3 min following puncture are collected as healing performance parameters. For the neat materials, the same tests are then repeated on gamma-ray irradiated samples to study the variation in self-repairing performance after exposure to simulated space radiation. Results show that the healing performance is higher in systems with lower viscous response and that it decreases after irradiation. A further analysis of the effects of space environment on the presented materials is hence required.

The NASA HZETRN2015 (High Z and Energy TRaNsport, 2015 version) software is also used to simulate the action of galactic cosmic rays on the space suit during extravehicular activity. The classic suit multilayer is compared with configurations in which the standard bladder is replaced with a layer of each analyzed material to identify the most promising candidates and determine whether the addition of nanofillers significantly increases the shielding ability.

1. Introduction

Space suits have been used to protect astronauts from space hazards for more than 50 years [1], but they will need to increase their protection ability in the framework of future space missions that will be related to longer exposure times of crewmembers. In particular, possible cuts and punctures generated by impacts with micrometeoroids and orbital debris (MMOD) could lead to their depressurization, a significant and eventually fatal issue for long-term crewed missions [2]. An effective solution to deal with impacts and enhance the lifetime and safety of space suits could be the insertion of self-healing polymers, but their properties could in turn be strongly modified by the space environment [3]. An example is given by possible degradation due to exposure to ionizing radiation from Galactic Cosmic Rays (GCR), Solar Particle Events (SPE) and Van Allen Belts [4]. Radiation must in fact be

* Corresponding author.
E-mail addresses: laura.pernigoni@polimi.it (L. Pernigoni), ugo.lafont@esa.int (U. Lafont), antoniomattia.grande@polimi.it (A.M. Grande).

https://doi.org/10.1016/j.actaastro.2023.05.032
Received 15 February 2023; Received in revised form 19 May 2023; Accepted 22 May 2023
Available online 27 May 2023

Nomenclature

Q	ICRP-60 quality factor
Q_{max}	maximum flow rate after puncture test
Q_{min}	minimum flow rate after puncture test
S_j	stopping power of a particle j
V_{leak}	volume leaked within 180 s after puncture
Δt	time between Q_{max} and Q_{min}
φ	solar modulation parameter

Acronyms/Abbreviations

ATR	attenuated total reflection
CNT	carbon nanotubes
DGEBA	diglycidyl ether of bisphenol A
DSC	differential scanning calorimetry
EMU	extravehicular mobility unit
FTIR	Fourier-transform infrared spectroscopy
GCR	galactic cosmic rays
HZETRN2015	High Z and Energy TRaNsport, 2015 version
ICRP	International Commission on Radiological Protection
ISS	International Space Station
LEO	Low Earth Orbit
MI	Methyl Imidazole
MMOD	micrometeoroids and orbital debris
MWCNT	multiwalled carbon nanotubes
NCRP	National Council on Radiation Protection
PUU	polyurea-urethane
SPE	solar particle event

contrasted through shielding due to its detrimental effects on material performance as well as human health. In particular, even if their effects on polymers in space still need to be fully determined, it was observed that GCR can change puncture extension and ultimate tensile strength and decrease ballistic performance as well as load-bearing capacity [5]. These aspects must hence be considered in the design of novel space suits and structures for future space missions [3,6], possibly relying on multifunctional materials with combined self-healing and radiation shielding properties. In these terms, different promising self-healing solutions were proposed in the last years. Examples related to protection against impacts and puncture are given by multilayer shields obtained from the combination of supramolecular polymers and ionomers with ripstop fabrics [7] and polymeric composites such as the one reinforced with E-glass and presented by Cohades and Michaud [8]. Additionally, vitrimers and vitrimer composites are also being considered for space due to their combined self-healing ability, recyclability, high chemical resistance and mechanical properties [9–11]. One of their future applications might be related to adhesives replacing bolted joints in spacecraft, with subsequent weight reduction [12]. Some polymers belonging to this class also possess good resistance to radiation: a study conducted by Meyer et al. on an aromatic thermosetting copolyester [12] showed in fact that this vitrimer did not experience significant surface chemistry changes after exposure to simulated Low Earth Orbit (LEO) radiation.

Different procedures have been followed and presented in literature to characterize the damage recovery performance and the response to space radiation of self-healing polymers. In the first case, high velocity impact tests [13–15] and low speed puncture tests [2] have been adopted. The repair ability of self-healing coatings was also studied by comparing their surface morphology through SEM analysis before and after scratching them [16]. The self-healing performance can also be determined by cutting a given sample in two and subsequently bringing its two halves into contact. Healing might be ensured through application of forces and/or heating for a given amount of time. Mechanical tests are then performed on undamaged and healed samples to compare them and determine the level of healing in terms of mechanical properties recovery [17].

As concerns the response to radiation, NASA conducted an extensive analysis on materials used in space, also considering a self-healing bladder concept [5]. Both numerical simulations and irradiation tests using different doses were performed focusing on different applications including an inflatable habitat and a space suit in deep space and in a Mars mission scenario. The considered doses were in Gy as the purpose was to analyze the degradation of materials rather than their ability to protect the human body, and spanned from 0.4 to 117 Gy.

What must be pointed out when looking at the here described studies is that some of them do not specifically focus on self-healing materials, and the remaining ones do not satisfactorily analyze the combined effect of mechanical damage and radiation on them. As concerns this second aspect, this combination might jeopardize the self-healing performance as it could significantly increase impact damage extension and rate [18]. As a consequence, there is currently limited information regarding the effectiveness and lifetime in space of self-healing materials, and a deeper knowledge of these aspects is required to determine if some of the available self-healing technologies can be used in space. Virtually no self-healing material has been space-qualified, and future research should focus on the understanding of the reliability and durability of self-healing systems in space, and on efficient testing and screening methodologies to assess their behavior in space.

The attempt of this research is to at least partially fill the gap in the currently available literature related to the issue of possible radiation-induced performance degradation of self-healing materials in space. In these terms, the self-healing performance of polyurea-urethanes (PUUs) and a supramolecular polymer with intrinsic autonomic self-healing properties is experimentally characterized and a preliminary estimate of the effects of simulated space radiation on these polymers is presented through irradiation tests. Furthermore, basic software simulations are run focusing on an extravehicular mobility unit (EMU) space suit case study to compare the shielding ability of these polymers with that of a standard suit bladder layer.

Nanocomposites with these polymers as matrices are also considered in both the experimental and the numerical part of this study as they are very appealing for space applications. In particular, polymeric nanocomposites typically possess higher mechanical, electrical and thermal properties than standard materials, are lighter and can be used in the creation of complex space structures with reduced waste generation in the related manufacturing process [19]. Recent studies also showed promising radiation shielding properties: for example, Li et al. [20] demonstrated that using a polymethyl methacrylate (PMMA) matrix containing multiwalled carbon nanotubes (MWCNTs) for a spacesuit application could lead to 2.4% reduction in neutron generation alongside a stunning 18% reduction in weight of the system. Furthermore, CNTs could be used to enhance both the mechanical properties and damage recovery ability of self-healing polymers [21,22]. Nevertheless, the difficulty in obtaining homogeneous dispersion of the nanofillers within a polymeric matrix still represents a relevant challenge alongside their selective functionalization [22]. This study also aims at looking for possible shielding performance improvements and modification to the healing ability of the considered polymers after adding MWCNTs to them.

The first part of this research focuses on puncture tests as a preliminary representation of MMOD impacts, analyzing their effect on different samples [2]. Bilayer and nanocomposite samples are investigated alongside reference neat polymer specimens. After the initial

puncture tests, some of the neat specimens are exposed to 100 Gy radiation doses before being tested again. A comparison is then made between pre and post irradiation results, to assess the possible changes of healing performance after exposure to radiation.

Finally, the NASA HZETRN2015 (High Z and Energy TRaNsport, 2015 version) software is used to simulate GCR acting on a space suit and have an initial idea about if and to what extent the considered solutions can improve the suit's shielding ability when used to replace the standard bladder layer [5]. The results are expressed in terms of absorbed equivalent dose as a function of the material's depth. Some of the neat materials are initially compared to find the ones with the best intrinsic properties, and then an attempt to further increase shielding is performed through insertion of nanofillers. Here GCR simulations are performed again, and the contribution of the nanofillers to the shielding properties is evaluated.

2. Materials and methods

2.1. Self-healing polymers

Four PUUs with similar formulation and fixed disulfide content but different crosslinking densities are analyzed (Table 1). They are obtained from different combinations of trifunctional and difunctional isocyanate-terminated pre-polymers PU-6000 and PU-4000, organized into networks connected by aromatic disulfides linkages and containing urea related H-bonds [23]. These pre-polymers are obtained from the interaction between poly (propylene glycol) and isophorone diisocyanate in the presence of the dibutyltin dilaurate catalyst [24].

The supramolecular polymer Reverlink® is also considered. It contains both covalent bonds and supramolecular hydrogen-bonding crosslinks (50:50 mol%). It is obtained from the combination of supramolecular pre-polymer SP-50, diglycidyl ether of bisphenol A (DGEBA) resin and 2-Methyl Imidazole (2-MI) catalyst, with nominal proportions reported in Table 2 [25,26]. The non-cured material is heated to 90 °C, poured into a Teflon® mold with a diameter of 60 mm and then cured at temperatures in the 120–150 °C range. Its glass transition temperature is between 5 °C and 15 °C [27,28]. For the sake of simplicity, this material will be from now on indicated with the HN-50 label.

2.2. Nanocomposites and bilayers

Nanocomposites with self-healing polymeric matrix and Nanocyl® NC7000™ MWCNTs [29] are considered as they could reduce the dose of incoming radiation reaching an astronaut while wearing an EMU suit.

Bilayer solutions are also analyzed to investigate possible healing performance improvements given by coupling the polymers with an additional layer (a 0.63 mm-thick aramid fabric or a 1.6 mm-thick silicone elastomer).

2.3. Samples manufacturing and puncture tests

Examples of specimens are shown in Fig. 1. The HN-50 samples have a nominal diameter of 60 mm and variable thickness, while the PUU ones have a nominal diameter of 20 mm.

As concerns the fabrication of the neat samples, the steps already presented in section 2.1 are followed to obtain the neat HN-50 specimens: mixing of precursors, pouring of the mixture into a Teflon® mold and curing at 120–150 °C. For the PUUs, smaller samples are cut from already available material slabs.

In the aramid/HN-50 configuration the uncured mixture obtained following the first mixing step for the manufacturing of HN-50 is poured on top of the aramid fibers, while for the other bilayers the final neat polymers are re-heated and coupled with the elastomer by applying pressure on the layers. 1 mm-thick polymeric layers are used in the PUU bilayer case. For the sake of clarity, the elastomer/HN-50 bilayer will be here indicated with the ME label.

As concerns the nanocomposites, in the experimental phase only samples with HN-50 matrix are manufactured and tested. The fabrication is divided into three basic steps: mixing of the MWCNTs (weight concentrations from 0.1% to 1%) with the uncured polymer resin, pouring of the mixture on the Teflon® mold, and curing at 120 °C for 24 h. The chosen mixing method combines magnetic stirring and bath sonication, obtained with a Branson® 2210R-MT ultrasonic bath, a Steinel® HG 2320-E heat gun and a VELP® ARE heated magnetic stirrer. Solvent dispersion is discarded because the related difficulty in properly removing solvent residuals [30] could lead to potential dangers in space applications.

All samples are treated with a 24-h drying cycle to remove humidity and then inserted between two polyamide films. This configuration is mounted on a system used to evaluate the self-healing performance through puncture tests and subsequent acquisition of the resulting leakage flow rate (Fig. 2). The samples are fixed on the central cylindrical part of the device and pressurized to a relative pressure of 30 kPa. Continuous air supply is provided to reproduce the reference case study represented by the internal environment of an EMU space suit. A vertical sinusoidal motion is imposed to the puncheon by the MTS 858 Mini Bionix® II machine (Fig. 3). An amplitude of 9.62 mm and 0.14 Hz frequency are set to obtain a velocity of 8.467 mm/s when the puncheon penetrates the specimen, coherently with the ASTM F1342/F1342M – 05 standard. Each specimen is tested three times, and maximum and

Table 1
PUUs formulations and basic properties [23].

Sample	Composition* [wt%]		ν [10^{-4} mol/cm^3]	T_g [°C]
PUU	PU-6000	PU-4000		
100	93.8	0	2.35	−58.8
90	84.4	9.4	2.05	−59
80	75.1	18.7	1.77	−59.4
70	65.7	28.1	1.50	−60.1

* Linker wt%: 6.2

Table 2
Reverlink® (HN-50) components [25].

Component	SP-50	DGEBA	2-MI
Mass [g]	23.900	6.020	0.004

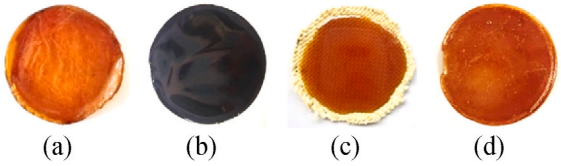

Fig. 1. Specimens examples - (a) Neat polymer, (b) nanocomposite and (c) (d) bilayers.

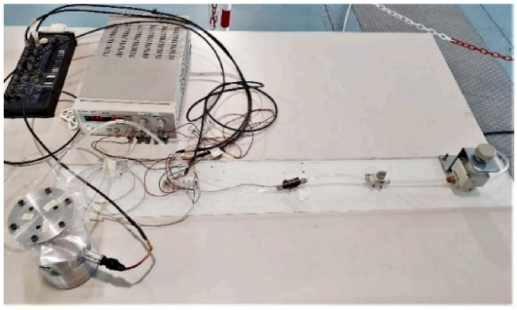

Fig. 2. Testing system.

Fig. 3. MTS 858 Mini Bionix® II machine for puncture tests.

minimum flow rates, the time between them and the air volume lost within 3 min from the puncturing event are collected as self-healing performance indicators. The choice of looking at the self-healing response within a short time interval (180 s) is dictated by the need of space materials able to recover from damage as fast as possible. As a matter of fact, a good but excessively slow healing response would be ineffective in an EMU space suit, as it would lead to fatal consequences for the astronauts.

2.4. Experimental setup for irradiation

Undamaged neat PUU samples are exposed to 100 Gy radiation doses emitted at 11.1 Gy/min rate by a Cobalt-60 source placed at a distance of 60.96 cm from the target. The 100 Gy dose chosen for these preliminary irradiation tests is taken from a reference study focusing on radiation in LEO [31]. This value is considered relevant for the analysis of possible effects on the materials in an EMU space suit used for extravehicular activities in an environment comparable to that outside the International Space Station (ISS). It is also comparable to the maximum dose considered in the study presented by NASA in Ref. [5], reproducing 50-year SPE exposure of the Vectran® layer in the inflatable habitat layup proposed in the report.

The irradiation process is performed in air, and the samples are subsequently stored in a cold room until the time of puncture tests to preserve chemical bonds deterioration generated by exposure to gamma rays.

2.5. Numerical irradiation simulations

The standard EMU space suit multilayer configuration (Table 3), used as a benchmark, is initially compared to two configurations in which the common bladder (layer 5) is replaced by HN-50 and PUU 100 respectively. In a second phase, nanocomposite solutions are also considered. The simulations are described in more detail in sub-subsections 2.5.1 and 2.5.2.

Table 3
Standard EMU space suit layers [5].

Layer[a]	Thickness (cm)	Name	Materials	Thickness (g/cm^2)
1	0.027	Orthofabric	50% Goretex 43% Nomex 6.25% Kevlar	0.049
2	0.01	Aluminized Mylar	Aluminum Mylar	0.00003 0.01399
3	0.025	Neoprene coat. Nylon	Nylon Neoprene	0.0078 0.022
4	0.015	Dacron	Dacron	0.021
5	0.028	Urethane coat. Nylon	Nylon Urethane	0.0078 0.022
6	0.135	Nylon	Nylon	0.154
Tot.	0.24			0.2976

[a] From outermost (1) to innermost (6). (5) = bladder.

The HZETRN2015 software tool [32] is used to simulate irradiation of the analyzed configurations under solar minimum conditions (maximum GCR intensity, low probability of SPE occurrence). A multilayer slab geometry with normally incident environment boundary conditions is considered, and the focus is set on dose equivalents absorbed by human tissue when shielded by the suit. The purpose is to understand whether the self-healing solutions lead to a better shielding of astronauts wearing the EMU, which would result in lower absorbed doses and improved protection of the crewmembers.

2.5.1. Neat polymers

In the first set of simulations the standard EMU configuration and the two EMU multilayers with neat PUU 100 and HN-50 replacing the standard bladder are irradiated with GCR in solar minimum conditions ($\varphi = 400$ MV). The resulting curves representing the total dose equivalents in human tissue are analyzed and compared. A multilayer slab geometry is considered.

2.5.2. Nanocomposites

The responses to radiation of EMU configurations containing nanocomposite bladders with HN-50 and PUU 100 matrices and different MWCNT contents are studied and compared to find the filler's concentration leading to the highest overall performance and its correlation with the shielding properties.

The 1%, 5% and 10% CNT weight percentages are analyzed, keeping in mind the 20% upper threshold dictated by practical limitations while processing the composites [33]. The standard EMU configuration is once again considered as a benchmark.

As in the neat case, the total dose equivalents in tissue from GCR exposure in solar minimum conditions are obtained and compared.

3. Theory and calculation

3.1. GCR simulations

As regards the simulation of GCR in HZETRN2015, the updated Badhwar-O'Neill model is used to generate the spectra of the related ions [34]. The solar modulation parameter φ is chosen as an input and set to 400 MV (solar minimum).

The total dose equivalents are the output of the simulations chosen to assess the stochastic effects of radiation on the human body (e.g.: cancer mortality, genetic damage). The absorbed doses in Gy are converted into equivalent doses in Sv through the ICRP-60 quality factor Q, which is recommended by the National Council on Radiation Protection (NCRP) [35]. This factor is a function of $S_j = S_j(E)$, which is the stopping power in keV/μm of a charged particle j at energy E in a material, tissue, or organ (Eq. (1)) [35]:

$$Q(S_j) = \begin{cases} 1 & 0 < S_j \leq 10 \\ 0.32S_j - 2.2 & 10 < S_j \leq 100 \\ \dfrac{300}{\sqrt{S_j}} & S_j > 100 \end{cases} \quad (1)$$

The equivalent doses are hence computed for each particle j by converting the absorbed doses through $Q(S_j)$, and are then summed up to obtain the total equivalent dose.

The equivalent dose per day in tissue is analyzed as a function of the depth in the EMU suit, considering that for the same thickness lower absorbed doses are related to better shielding performance [35]. Thicknesses are indicated in g/cm^2 (cumulative areal density), as usually done in radiation analysis. In the case under study this doesn't introduce relevant inaccuracies or discrepancies in the results when

moving from areal thickness to proper thickness in cm, as the densities of the materials considered in the bladder (standard materials, HN-50 and PUU 100) are all comparable and close to 1 g/cm^3.

4. Results and discussion

4.1. Puncture tests on non-irradiated samples

Focusing on the nanocomposite samples, the puncture tests show that self-healing is mainly related to the specimen's thickness rather than to the concentration of MWCNTs. Furthermore, complete healing is not reached, and practical issues are also encountered when trying to increase the concentration of nanotubes, making this solution less appealing than the bilayers. For the sake of clarity, Fig. 4 shows the experimental data for the 1% MWCNT configuration as a reference example.

As concerns the bilayer configurations, while the aramid fabric does not provide significant improvements the polymer/elastomer coupling on the other hand increases the self-healing performance. As a matter of fact, the elastomer's springback behavior accelerates the self-healing process by promoting hole closure in the punctured region (Fig. 5 for the ME configuration, Fig. 6 showing the example of PUU 100, taken as representative of the related family of polymers). The bilayer configuration containing the PUU 90 polymer is characterized by the highest average performance (Table 4), which is in contrast with the neat polymers results. In the neat configuration PUU 100 has in fact the best overall performance, probably due to its strong springback response which ensures short healing times and reduced air leakage after perforation. This discrepancy between the bilayer and neat cases might be due to repeatability issues in the experiments and needs to be further investigated.

4.2. Puncture tests on irradiated samples

Comparison of average results for irradiated and blank (non-irradiated) PUU samples of the same type and thickness shows that deterioration of the healing performance is already visible for a dose of 100 Gy. In general, stronger degradation is observed in materials with higher concentrations of difunctional units. The neat PUU 100 samples results are displayed as a reference example in Table 5 and Fig. 7, also because they have the highest healing performance in the blank neat case, as stated in section 4.1.

ATR FTIR and DSC characterization of the neat samples are also performed alongside the puncture tests to compare blank and irradiated samples and look for possible changes in the material properties due to radiation. The related results can be found in the Supporting

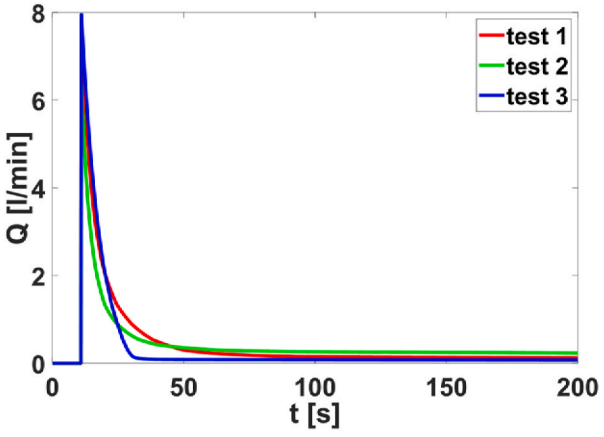

Fig. 4. Puncture test results for the MWCNT nanocomposite with HN-50 matrix.

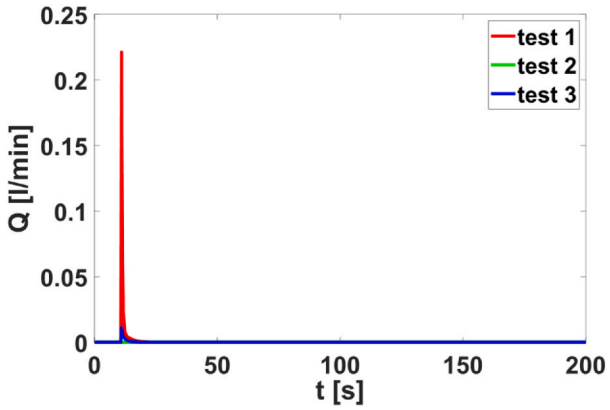

Fig. 5. Puncture test results for the ME configuration (HN-50/elastomer bilayer).

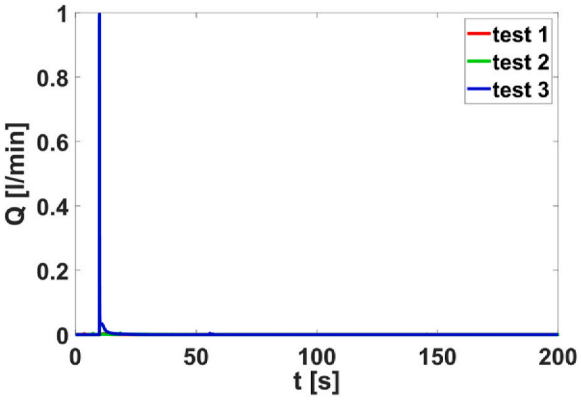

Fig. 6. Puncture test results for the PUU 100-elastomer bilayer.

Table 4
Average results for elastomeric bilayer and nanocomposite specimens compared to the study presented by NASA in Ref. [36].

Sample	Q_{max} [l/min]	Q_{min} [l/min]	Δt [s]	V_{leak} [l]
Bilayer with elastomer				
ME	0.0777	0	7.96	0.0005
PUU 70	0.4017	0	99.62	0.0059
PUU 80	0.1860	0	11.44	0.0020
PUU 90	0.0411	0	9.08	0.0004
PUU 100	0.3352	0	10.47	0.0012
Nanocomposite				
1% CNT	7.3830	0.1423	200.00	1.2519
NASA 1998 study [36]				
Bladder	2.4010	1.032	300.50	3.8968
Conathane®	0.2080	0.054	110.00	0.2273
TyrLyner® urethane	4.5230	0.085	153.75	0.5422
Sylgard®	2.7000	0.455	366.35	2.4189

Table 5
Puncture tests results for irradiated and non-irradiated neat PUU 100 samples.

Sample	Q_{max} [l/min]	Q_{min} [l/min]	Δt [s]	V_{leak} [l]
Irradiated				
1	2.8231	0.0281	189.69	0.1453
2	3	0.0171	189.57	0.1003
3	2.6221	0.0503	188.61	0.2861
Non irradiated				
1	1.2549	0	5.66	0.0025
2	1.7352	0.0147	189.80	0.1057
3	1.5489	0	4.84	0.0017

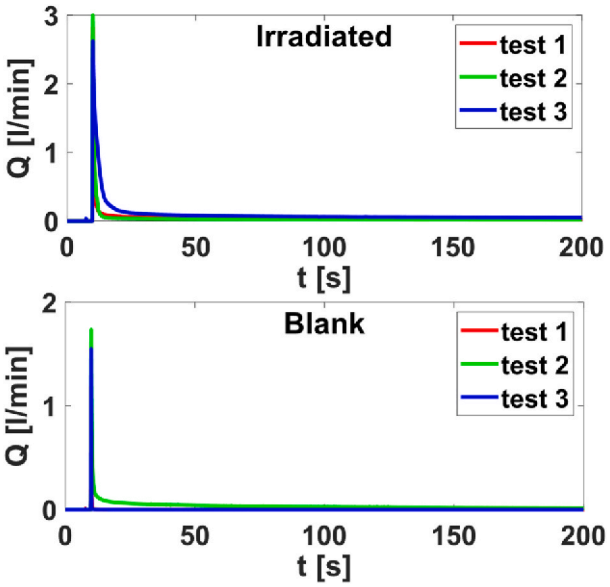

Fig. 7. Puncture tests comparison for irradiated and blank (non-irradiated) neat PUU 100 samples.

Information and will not be included in the main article as no relevant changes are found after irradiation in the spectra and in the DSC curves and glass transition temperatures of the materials.

4.3. Simulated irradiation on neat polymers

Figs. 8 and 9 show the comparison of the results from simulated GCR irradiation of the space suit configurations with neat polymers. Being the shielding properties similar within the different PUUs, for the sake of clarity PUU 100 is chosen as the representative material and only the dose curves related to it are displayed in the plots. Moving from left to right in these plots, the curves go from the outermost (1) to the innermost (6) layer of the suit. The equivalent dose at a given thickness is the value that would be absorbed by human tissue if it was shielded only by the layers in the plot region to the left of the considered thickness value.

As expected, the curves in Fig. 8 and in Fig. 9 are identical up until the bladder, since the four outermost layers of the space suit remain unchanged when switching from the standard to the self-healing configuration. From layer 5 on, a discrepancy appears among the absorbed dose equivalent values.

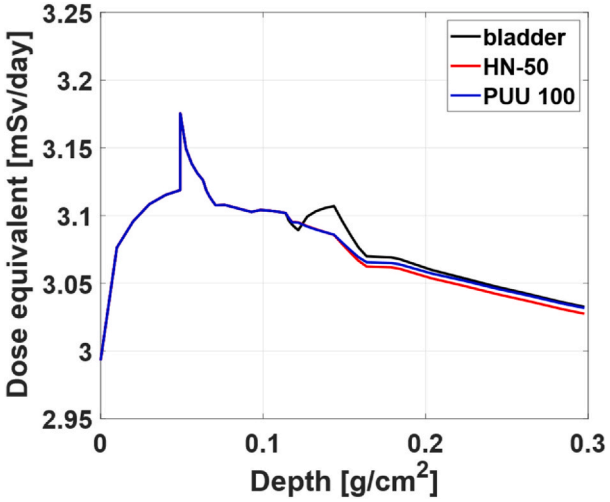

Fig. 8. Total equivalent doses, neat case.

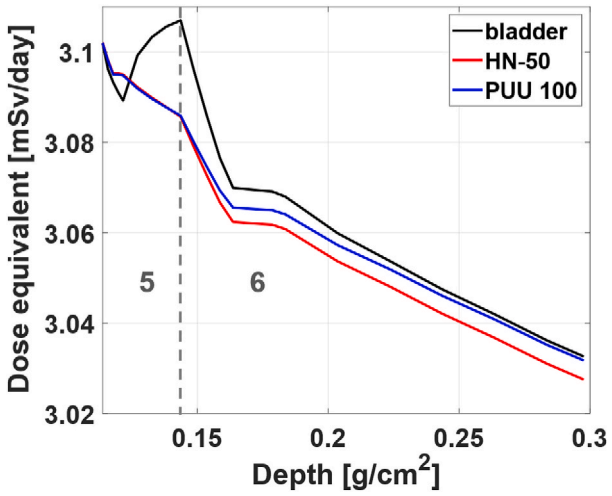

Fig. 9. Total equivalent doses, neat case, zoom on layers 5 (bladder) and 6.

As lower doses at the same thickness indicate better radiation shielding [15], it is observed that the HN-50 configuration is the one with the highest performance, followed by the PUU setup and the standard space suit multilayer. The relevant dose value to be considered is the one related to the 0.2976 g/cm^2 overall areal thickness of the suit, as it indeed represents the dose absorbed by human tissue shielded by the space suit in its entirety. Even though the improvement in the shielding ability is rather limited, these results are anyway very important. As a matter of fact, they show that replacing the standard bladder with a self-healing equivalent not only gives the space suit the additional ability to autonomously repair, but it also slightly increases its shielding performance against GCR.

A general objection that could be made is that at a given cumulative areal density different materials are typically related to different equivalent thicknesses in cm due to their different densities. This could result in possible errors in determining the actual dose at a given thickness in cm [35]. Nevertheless, as the materials considered for the bladder options have similar densities, replacing the standard bladder with a PUU 100 or HN-50 layer with the same areal density can be considered equivalent to doing so with thicknesses in cm. The dose-versus-areal density curves can hence be directly used to compare the results without introducing relevant inaccuracies.

4.4. Simulated irradiation on nanocomposites

The results of the HZTERN2015 simulations are consistent with the neat polymers outcomes: once again, the nanocomposites with HN-50 matrix give the best shielding response (Fig. 10). As a matter of fact, no actual relevant improvement to the overall radiation shielding performance is observed when comparing the neat self-healing polymers to the related nanocomposites. The HN-50 case is shown in Fig. 11, and the same applies for PUU 100. In the here studied case the high cost, complexity and manufacturing challenges related to the nanocomposites hence lead to the idea of discarding them in favor of the much more affordable and easier to implement neat configurations.

5. Conclusions

The puncture tests presented in this research ~~phase~~ show that the polymer/elastomer layer coupling leads to significant improvements with respect to previous studies, with null minimum flow rates and fast sealing times reached in all the tests. The performance of this configuration could be further increased through a trade-off between thickness reduction and preservation of the self-healing properties. Furthermore, optimal healing performance could be ensured in the neat materials by a

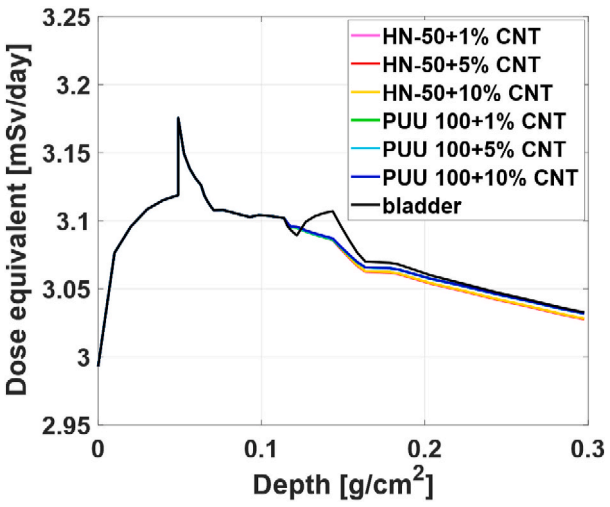

Fig. 10. Total equivalent doses, nanocomposites.

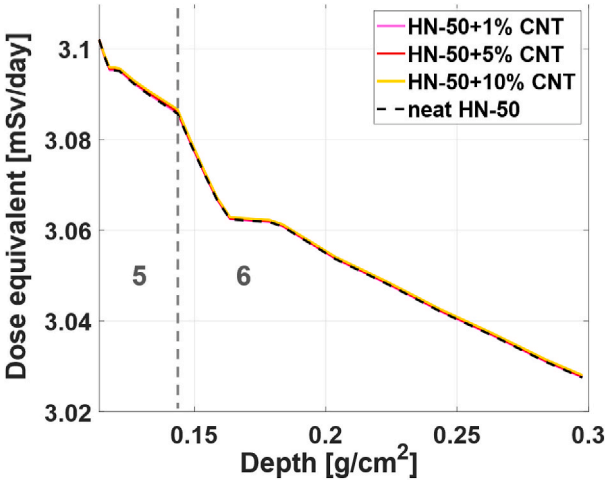

Fig. 11. Compared neat material and nanocomposite doses for HN-50, layers 5 (bladder) and 6.

good trade-off between elastic and viscous behavior, as the former allows fast contact between the edges of a damaged area, and the latter is required for sealing. Overall, the most promising solution is the bilayer configuration coupling the elastomer with PUU 90. As concerns the effects of space radiation, doses of the order of 100 Gy seem to already compromise the materials' healing performance.

The HZETRN2015 simulations from the last part of this study show that integration of HN-50 into an EMU space suit as the bladder layer leads to the highest overall shielding performance. Furthermore, as the subsequent insertion of nanofillers into HN-50 and PUU 100 does not significantly increase their radiation shielding ability, it is chosen to stick with the more convenient and affordable neat solutions.

As a general conclusion, a self-healing layer could indeed significantly increase safety, reliability, and lifetime of space suits for future missions, but further studies must be carried out to successfully implement this solution.

As a future step, the here used slab geometry approach could be replaced by 3D numerical analysis to obtain more accurate results. To get an initial estimate of the operational life of the materials, a complete mission should also be simulated to analyze the doses absorbed at each mission phase (e.g.: EVAs, transfer route, permanence on the surface of a planet or satellite) by the space suit, or even by a different multilayer space structure such as a habitat.

Finally, another important and necessary step is a more accurate and complete experimental characterization of part of the analyzed materials under simulated space radiation environment to analyze if and how their mechanical, self-healing, chemical and physical properties degrade in space.

Declaration of competing interest

The authors declare that they have no known competing financial interests or personal relationships that could have appeared to influence the work reported in this paper.

Acknowledgements

This research was supported by ESA, contract No. 4000132669/20/NL/MH/ic. The authors are grateful to Arkema for supplying Reverlink®, and to Prof. Mario Mariani and the Radiochemistry and Radiation Chemistry Laboratory at Politecnico di Milano for the help with the irradiation tests. Special thanks go to Alberto Sironi for the help provided with the HZETRN2015 tool.

Appendix A. Supplementary data

Supplementary data to this article can be found online at https://doi.org/10.1016/j.actaastro.2023.05.032.

References

[1] D.P. Cadogan, The past and future space suit, Am. Sci. 103 (2015) 338–348.
[2] L. Pernigoni, A.M. Grande, Development of a supramolecular polymer based self-healing multilayer system for inflatable structures, Acta Astronaut. 177 (2020) 697–706, https://doi.org/10.1016/j.actaastro.2020.08.025.
[3] L. Pernigoni, U. Lafont, A.M. Grande, Self-healing Materials for Space Applications: Overview of Present Development and Major Limitations, CEAS Sp. J., 2021, https://doi.org/10.1007/s12567-021-00365-5.
[4] J. Rask, W. Vercoutere, B.J. Navarro, A. Krause, Space Faring: the Radiation Challenge, an Interdisciplinary Guide on Radiation and Human Space Flight, 2008.
[5] J.M. Waller, K. Rojdev, K. Shariff, D.A. Litteken, R.A. Hagen, Simulated Galactic Cosmic Ray and Solar Particle Event Radiation Effects on Inflatable Habitat , Composite Habitat, Space Suit and Space Hatch Cover Materials, 2020.
[6] S.K. Ghosh (Ed.), Self-healing Materials-Fundamentals, Design Strategies, and Applications, Wiley-VCH, 2009.
[7] E. Haddad, Y. Zhao, M. Celikin, M. Basti, K. Tagziria, E. Wallach, C. Semprimoschnig, U. Lafont, I. McKenzie, Mitigating the effect of space small debris on COPV in space with fiber sensors monitoring and self-repairing materials, in: Z. Sodnik, N. Karafolas, B. Cugny (Eds.), ICSO Proc., ESA and CNES, Chania, 2018, https://doi.org/10.1117/12.2536183.
[8] A. Cohades, V. Michaud, Damage recovery after impact in E-glass reinforced poly (ε-caprolactone)/epoxy blends, Compos. Struct. 180 (2017) 439–447, https://doi.org/10.1016/j.compstruct.2017.08.050.
[9] J.L. Meyer, M. Bakir, P. Lan, J. Economy, I. Jasiuk, G. Bonhomme, A.A. Polycarpou, Reversible bonding of aromatic thermosetting copolyesters for in-space assembly, Macromol. Mater. Eng. 304 (2019) 1–9, https://doi.org/10.1002/mame.201800647.
[10] M. Röttger, T. Domenech, R. Van Der Weegen, A. Breuillac, R. Nicolaÿ, L. Leibler, High-performance vitrimers from commodity thermoplastics through dioxaborolane metathesis, Science 356 (2017) 62–65, https://doi.org/10.1126/science.aah5281, 80-.
[11] D.J. Fortman, J.P. Brutman, C.J. Cramer, M.A. Hillmyer, W.R. Dichtel, Mechanically activated, catalyst-free polyhydroxyurethane vitrimers, J. Am. Chem. Soc. 137 (2015) 14019–14022, https://doi.org/10.1021/jacs.5b08084.
[12] J.L. Meyer, P. Lan, S. Pang, K. Chui, J. Economy, I. Jasiuk, Reversible bonding via exchange reactions following atomic oxygen and proton exposure, J. Adhes. Sci. Technol. 0 (2021) 1–18, https://doi.org/10.1080/01694243.2021.1876403.
[13] K.L. Gordon, E.J. Siochi, W.T. Yost, P.B. Bogert, P.A. Howell, K.E. Cramer, E. R. Burke, Ballistic Puncture Self-Healing Polymeric Materials, 2017, pp. 1–21.
[14] K. Gordon, R. Penner, P. Bogert, W.T. Yost, E. Siochi, Puncture self-healing polymers for aerospace applications, in: 242nd Am. Chem. Soc. Natl. Meet. Expo., 2011.
[15] S.R. Zavada, N.R. McHardy, K.L. Gordon, T.F. Scott, Rapid, puncture-initiated healing via oxygen-mediated polymerization, ACS Macro Lett. 4 (2015) 819–824, https://doi.org/10.1021/acsmacrolett.5b00315.
[16] Y. Zhu, K. Cao, M. Chen, L. Wu, Synthesis of UV-responsive self-healing microcapsules and their potential application in aerospace coatings, ACS Appl. Mater. Interfaces 11 (2019) 33314–33322, https://doi.org/10.1021/acsami.9b10737.

[17] K. Yu, A. Xin, H. Du, Y. Li, Q. Wang, Additive manufacturing of self-healing elastomers, NPG Asia Mater. 11 (2019), https://doi.org/10.1038/s41427-019-0109-y.
[18] E. Grossman, I. Gouzman, Space environment effects on polymers in low earth orbit, Nucl. Instrum. Methods Phys. Res. B. 208 (2003) 48–57, https://doi.org/10.1016/S0168–583X(03)00640-2.
[19] A. Bhat, S. Budholiya, S. Aravind Raj, M.T.H. Sultan, D. Hui, A.U. Md Shah, S.N. A. Safri, Review on nanocomposites based on aerospace applications, Nanotechnol. Rev. 10 (2021) 237–253, https://doi.org/10.1515/ntrev-2021-0018.
[20] Z. Li, S. Chen, S. Nambiar, Y. Sun, M. Zhang, W. Zheng, J.T.W. Yeow, PMMA/MWCNT nanocomposite for proton radiation shielding applications, Nanotechnology 27 (2016), 234001, https://doi.org/10.1088/0957-4484/27/23/234001.
[21] Z.-W. An, R. Xue, K. Ye, H. Zhao, Y. Liu, P. Li, Z.-M. Chen, C.-X. Huang, G.-H. Hu, Recent advances in self-healing polyurethane based on dynamic covalent bonds combined with other self-healing methods, Nanoscale 15 (2023) 6505–6520, https://doi.org/10.1039/D2NR07110J.
[22] R.V.S.P. Sanka, B. Krishnakumar, Y. Leterrier, S. Pandey, S. Rana, V. Michaud, Soft self-healing nanocomposites, Front. Mater. 6 (2019), https://doi.org/10.3389/fmats.2019.00137.
[23] A.M. Grande, R. Martin, I. Odriozola, S. van der Zwaag, S.J. Garcia, Effect of the polymer structure on the viscoelastic and interfacial healing behaviour of poly (urea-urethane) networks containing aromatic disulphides, Eur. Polym. J. 97 (2017), https://doi.org/10.1016/j.eurpolymj.2017.10.007.
[24] A. Rekondo, R. Martin, A. Ruiz de Luzuriaga, G. Cabañero, H.J. Grande, I. Odriozola, Catalyst-free room-temperature self-healing elastomers based on aromatic disulfide metathesis, Mater. Horiz. 1 (2014) 237–240, https://doi.org/10.1039/C3MH00061C.
[25] D. Montarnal, F. Tournilhac, M. Hidalgo, L. Leibler, Epoxy-based networks combining chemical and supramolecular hydrogen-bonding crosslinks, J. Polym. Sci. Part A Polym. Chem. 48 (2010) 1133–1141, https://doi.org/10.1002/pola.
[26] F. Sordo, S.J. Mougnier, N. Loureiro, F. Tournilhac, V. Michaud, Design of self-healing supramolecular rubbers with a tunable number of chemical cross-links, Macromolecules 48 (2015) 4394–4402, https://doi.org/10.1021/acs.macromol.5b00747.
[27] F. Sordo, V. Michaud, Processing and damage recovery of intrinsic self-healing glass fiber reinforced composites, Smart Mater. Struct. 25 (2016), 084012, https://doi.org/10.1088/0964-1726/25/8/084012.
[28] Arkema, Reverlink supramolecular technology , (n.d.) 1–8.
[29] Nanocyl, NC7000™–Technical Data Sheet, 2021.
[30] I. Gouzman, E. Grossman, R. Verker, N. Atar, A. Bolker, N. Eliaz, Advances in polyimide-based materials for space applications, Adv. Mater. 31 (2019) 1–15, https://doi.org/10.1002/adma.201807738.
[31] M. Anderson, A.N. Zagrai, J.D. Daniel, D.J. Westpfahl, D. Henneke, Investigating effect of space radiation environment on piezoelectric sensors: cobalt-60 irradiation experiment, J. Nondestruct. Eval. Diagnostics Progn. Eng. Syst. 1 (2018), https://doi.org/10.1115/1.4037684.
[32] NASA, HZETRN2015 User Guide (2015).
[33] S. Laurenzi, G. de Zanet, M.G. Santonicola, Numerical investigation of radiation shielding properties of polyethylene-based nanocomposite materials in different space environments, Acta Astronaut. 170 (2020) 530–538, https://doi.org/10.1016/j.actaastro.2020.02.027.
[34] P.M. O'Neill, Badhwar–O'Neill galactic cosmic ray model update based on advanced composition explorer (ACE) energy spectra from 1997 to present, Adv. Space Res. 37 (2006) 1727–1733, https://doi.org/10.1016/j.asr.2005.02.001.
[35] R.C. Singleterry, Radiation engineering analysis of shielding materials to assess their ability to protect astronauts in deep space from energetic particle radiation, Acta Astronaut. 91 (2013) 49–54, https://doi.org/10.1016/j.actaastro.2013.04.013.
[36] T.H. Fredrickson, NASA Research Announcement Final Report for Space Suit Survivability Enhancement, 1998.